

Regulatory context of smart grids in Europe and Brazil: current state and trends

Third ELECON Workshop

University of Grenoble Alps – G2ELab, Grenoble, France, November 17-18, 2015.

Joint linear modelling of the load demand and thermal behavior of a smart building

Vincent Reinbold^a, Daniel Tenfen^b, Van-Binh Dinh^a

^bUniv. Grenoble Alpes, G2ELab, F-38000 Grenoble, France

^aUFSC, Campus Universitário - CTC, Florianópolis - CEP: 88040-900, Brazil

Abstract

This paper presents a mathematical model for load demand, batteries and thermal envelop of the building to the Energy Management (EM) problem of a Microgrid (MG) by means of a deterministic Mixed Integer Linear Programming (MILP) approach. This way, the thermal envelop of the building can be seen as a load demand and thermal storage. In the EM problem, the objective is to determine a generation and consumption policy that minimises, over a planning horizon, the operation cost and the thermal comfort subject to economic and technical constraints. We propose a detail modelling of different load demands and Li-ion batteries. To analyse the proposed modelling, a didactic MG and simple thermal envelop of a building is used, connected to the main grid, although, the proposed models could also be used in the island operation. The results indicate that the models are adequate for the MG EM, analyses of the impacts and energies policies.

Keywords: Smart Building, Demand response, Real time pricing, linear modelling.

1. Introduction

The microgrid concept assumes a cluster of micro generation and loads operating as a single system [1]. The presence of this distribution energy resources (DERs) and controllable loads

reduces fossil fuel consumption and peak shaving. Operations issues in the microgrids are usually answered by a mixed integer linear programming to solve the energy management problem. In general, solving this problem requires determining a generation and a controllable load demand policy that minimizes, over a planning horizon, an objective function subject to economic and technical constraints [1-3].

The building sector is the most important consumer of energy in the world. In France, it also consumes 43% of primary energy and 66% of electrical energy of which the cooling and heating section accounts for 50%. In this point of view, the building can be seen as an important load of the smart grid. Moreover, the thermal capacity of the building could also play a particular role in the energy management of the microgrids.

Thermal envelope is usually simulated with dedicated software like *EnergyPlus* or *TRNSys*, which make the use of it difficult in a more general modelling.

The classical EM problem formulation usually takes into account economic objective linked to investments, energy cost or use [2-3]. But, the introduction of the thermal into the MG model involves other objectives like thermal comfort, air quality or lightning.

The main objective of this paper is to make a joint mixed integer linear programming of a smart building, his microgrid and his thermal envelope. The EM and the thermal modelling of the thermal envelope are obtained by a deterministic mixed-integer linear programming problem. The planning horizon is two weeks with one hour step time. This paper is organized as follow: the modelling of the microgrid in the next section. Thermal envelope modelling is described in section 4. In section 5 and 6, we present the global modelling of the smart building and the first results of the study.

2. Microgrid modelling

2.1. Main grid

The main grid is defined by minimal and maximal power (p_{min} and p_{out}). p_{out} is defined as the sold power from the microgrid to the maingrid. p_{in} is defined as the bough energy from the maingrid to the microgrid. That way, both of them are always positive. MILP formulation of the microgrid is defined as followed:

$$\forall t, p(t) = p_{in}(t) - p_{out}(t) \quad (1)$$

$$O_1 = \sum_t c_{in} \cdot p_{in}(t) + c_{out} \cdot p_{out}(t) \quad (2)$$

$$\forall t, p_{in}(t) < p_{max} \cdot u(t) \quad (3)$$

$$\forall t, p_{out}(t) < p_{min} \cdot (1 - u(t)) \quad (4)$$

$$\forall t, p_{in}(t), p_{out}(t) \in R^+, u(t) \in \{0; 1\} \quad (5)$$

where c_{in} and c_{out} are respectively the buying and the selling costs. One can see that the binary variable u prohibits selling and buying in the same time, *c.f.* (3) and (4). In the convex case ($c_{out} < c_{in}$), one can use the simpler LP formulation:

$$\forall t, p(t), c(t) \in \mathbf{R} \quad (1)'$$

$$O_1 = \sum_t c(t) \quad (2)'$$

$$\forall t, p_{min} < p(t) < p_{max} \quad (3)'$$

$$\forall t, c(t) > c_{in} \cdot p(t) \quad (4)'$$

$$\forall t, c(t) > c_{out} \cdot p(t) \quad (5)'$$

In this study, we are assuming fixed selling and buying prices : $c_{in} = 0.1048$, $c_{out} = -0.2096$.

2.2. Wind turbine and PV panels

The wind turbine is modeled as a fixed input. The generation input power P_w is computed thanks to the wind forecast as followed [4][6][7]:

$$p_w(t) = \begin{cases} 0 & \text{if } 0 < v(t) < v_c \text{ or } v(t) > v_f \\ p_r \cdot \frac{v(t) - v_c}{v_r - v_c} & \text{if } v_c < v(t) < v_r \\ p_r & \text{if } v_r < v(t) < v_f \end{cases} \quad (6)$$

where p_r is the rated electrical power; v_c is the cut-in wind speed; v_r is the rated wind speed; v_f and is the cut-off wind speed.

In the PV system, we assume that a maximum power point tracker will be used. The maximum power output is presented by [4][9]:

$$p_s(t) = \eta_s \cdot S \cdot I(t) \cdot (1 - 0.005 \cdot (t_{ext}(t) - 25)) \quad (7)$$

Where η is the conversion efficiency of the solar cell array (%), S is the array area (m^2); I is the solar radiation (kW/m^2) and t_{ext} is the outside air temperature ($^{\circ}C$).

2.3. Heating and cooling system

The case study include a 3kW electrical heating system and a 3kW (thermal) cooling system. We assume a complete control of this system (continuous power). For different products, one has to adapt the modelling adding variables and constraints. The thermal discomfort is added to the formulation by mean of a weighed term to be minimized. This discomfort is modelled as a weighed sum of deviations from a reference temperature T_{ref} as follow [5]:

$$O_2 = \sum_t c_c \cdot |t_{in}(t) - T_{ref}| \cdot \Delta t$$

where c_c is the cost of discomfort (euros/°C/h). This equation can be linearized as follow:

$$O_2 = \sum_t c_c \cdot (d_1(t) + d_2(t)) \cdot \Delta t \quad (8)$$

$$\forall t, d_1(t), d_2(t) \leq 0 \quad (9)$$

$$\forall t, d_1(t) - d_2(t) = t_{int}(t) - T_{ref} \quad (10)$$

Constraints for cooling and heating systems can be formulated as follow:

$$\forall t, \quad q_c(t) = \eta_c \cdot p_c(t) \quad (11)$$

$$\forall t, \quad p_h(t) < p_h^M \quad (12) \quad q_c(t) < q_c^M \quad (13)$$

where η_c is the cooling efficiency and q_c^M is the thermal maxim cooling power.

3. Thermal modelling

The main goal of the section is to present the study case and the thermal envelope modelling. This is a linear model, directly link to the electrical model of the microgrid. In this point of view, the thermal envelope can be seen as a thermal storage of energy. It is particularly interesting since the thermal envelope constitutes a great capacity compared to other classical storage like batteries.

3.1. Case Study

The case study is the building which is in the ADEME^a research project “COMEPOS^b” aiming at constructing twenty five positive energy buildings in France by 2018. This house is built with more than 200 m² of ground surface, one heated zone, one garage and two basements. It is designed with the good insulation materials to save the energy consumed by heating and air conditioning systems.

A first model (Figure 1) which enables the dynamic thermal simulation was developed by our partner LOCIE^c laboratory, using *EnergyPlus* software.

^a www.ademe.fr

^b www.comepos.fr/

^c www.polytech.univ-savoie.fr/locie

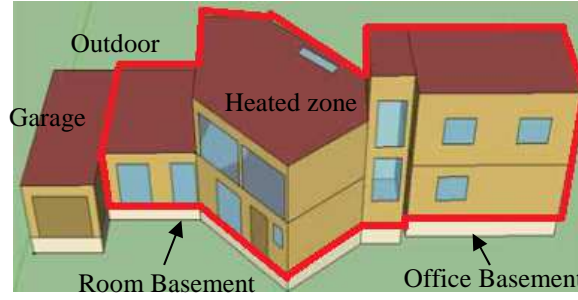
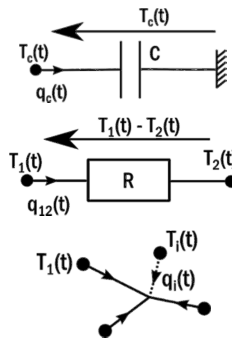


Figure 1 Energy Plus model

This model is considered as a reference model from which we built a reduced order model in the form of an equivalent circuit (9R5C) for optimization purpose.

3.2. Linear modelling and validation

Thermal envelope of the building is usually modelled with simple circuit components: resistances (conduction and convection) to model heat transfers and capacity to model the thermal capacity of wall and interior air. Those models are described by the figure XX. Note that capacity equations are solved by a simple Euler's method. Each connection in the thermal circuit are represented by the set of equations (10).



$$q_c(t) = C \cdot \frac{\partial T_c(t)}{\partial t} \approx C \cdot \frac{T_c(t) - T_c(t-1)}{\Delta t} \quad (14)$$

$$q_{12}(t) = \frac{T_1(t) - T_2(t)}{R} \quad (15)$$

$$\sum_i q_i(t) = 0 \quad \& \quad \forall i \quad T_i(t) = T_1(t) \quad (16)$$

The equivalent circuit (9R5C) is presented in Figure 2. This thermal circuit is based on passed works. Identifications of parameters has been done using an optimization procedure and the simulation result under EnergyPlus. We used data profile of one year for the identification then validated the parameters obtained for another year data. Identified parameters are given in Table 1.

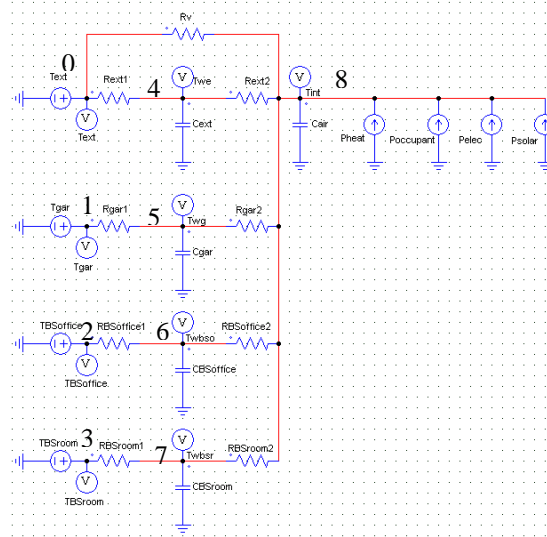


Figure 2 Electrical equivalent circuit

Parameters identified values

<i>Cair</i>	3747281.44	<i>Rgar1</i>	0.17195
<i>Cext</i>	38832547.60	<i>Rgar2</i>	0.16600
<i>Cgar</i>	233332.53	<i>Rv</i>	0.00738
<i>CBSoffice</i>	3038849.96	<i>RBSoffice1</i>	0.06713
<i>CBSroom</i>	8110949.64	<i>RBSoffice2</i>	0.01350
<i>Rext1</i>	0.00789	<i>RBSroom1</i>	0.12775
<i>Rext2</i>	0.00417	<i>RBSroom2</i>	0.00220

Table 1: Identified thermal parameters of the circuits

The heated zone is described with four walls, an internal air capacity and a thermal resistance representing the thermal resistance link to the ventilation. Each wall is described by two thermal resistances and a capacity. In the following, the ventilation is assumed to be constant ($0.13 \text{ m}^3/\text{h}$) to guaranty a good air quality and minimize heat losses. In the future, this shall be reformulated to ensure a variation of the air flow in order to allow the natural cooling of the room during the night for instance.

Temperatures of non-heated rooms are supposed to be fixed to simplify the modelling. These are fixed to the *EnergyPlus* simulations results to ensure a good agreement in the case of good temperature control.

One can see in Figure 2 that solar irradiation, heating/cooling input power, occupancy and electrical losses are taken into account as power inputs. Figure 3 shows power inputs with respect to the time for two weeks in January.

As a thermal validation, we are comparing the internal temperature between the *EnergyPlus* simulation and the linear model in Figure 4. To allow a good comparison of the thermal envelope, heating and cooling systems are turned off. One can see the good global agreement of both temperatures.

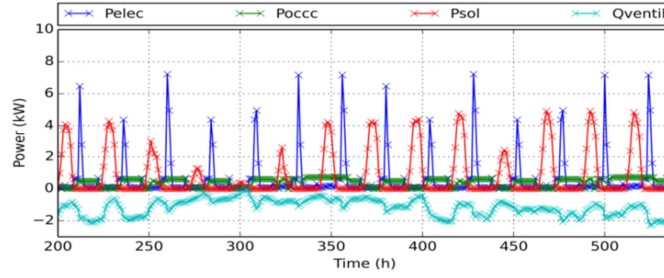


Figure 3 Power inputs for the thermal modelling

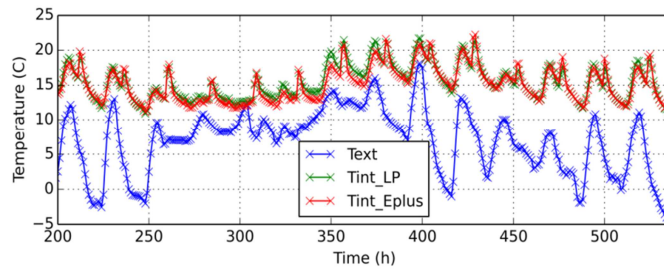


Figure 4 Internal temperature comparison between the LP model and EnergyPlus

4. Smart building modelling

4.1. The complete MILP formulation

The complete model for the smart building is obtained by the aggregation of the micro-grid and thermal model. It can be formulate as follow:

$$\min O = O_1 + O_2 + \sum_t (c_{de} \cdot p_{de}(t) + c_{ex} \cdot p_{ex}(t)) \cdot \Delta t \quad (17)$$

$$-p_h(t) - p_c(t) + p_w(t) + p_s(t) + p_{m,g}(t) - p_{elec}(t) = 0 \quad (18)$$

Main Grid : (1)-(5)

Wind turbine : (6)

PV panels : (7)

Heating and cooling systems : (8)-(13)

Thermal envelope : (14)-(16)

Equation (17) is composed by electricity and discomfort costs (2), (8), as well as artificial variables for deficit and excessive power generation. Equation (18) is the energy balance of the electrical grid. The energy balance in the thermal envelope is described by (16).

5. Results

The computational model is implemented in an oriented object way in Python 2.7. We use the Gurobi 6.0 to solve the optimization problem and tests are executed on an Intel Core CPU (T9600), 2.8 GHz with 3Go of RAM.

5.1. Temporal analysis for two different discomfort costs

To show the influence of the cost of discomfort introduced in the MILP formulation, we made different tests. Figures 5, 6 and 7 shows mains results for two different costs of discomfort ($cc = 0.25$ and 2.25 euros/ $^{\circ}\text{C}/\text{h}$) for two weeks in January.

Firstly, the figure 5 presents internal and external temperatures for both cases.

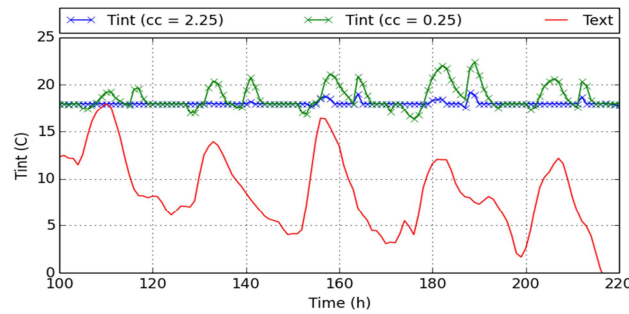


Figure 5 Internal temperature comparison for $cc = 0.25$ and 2.25 (euros/ $^{\circ}\text{C}/\text{h}$)

One can see that intern temperature control is different in both cases. For a low cost of discomfort, we note a bad control of temperature; indeed, the internal temperature can vary from 17 to 21 $^{\circ}\text{C}$ and leads to a mean temperature deviation of 0.58 $^{\circ}\text{C}$. In the second case, the high cost of discomfort, in comparison to the cost of energy (c_{in}), the optimization leads to a mean temperature deviation of 0.08 $^{\circ}\text{C}$.

C_c (euros/ $^{\circ}\text{C}/\text{h}$)	Mean thermal deviation ($^{\circ}\text{C}$)	Cost of electricity (euros)
2.25	0.08	94.6
0.25	0.58	20.9

Table 2 : Optimization results for $cc = 0.25$ and $cc = 2.25$ (euros/ $^{\circ}\text{C}/\text{h}$)

Figure 6 represents heating and cooling optimal control for both cases. In the high cost case, heating and cooling systems are used daily to ensure a perfect control of the internal temperature between cold and hot phases (day and night). Note that the cooling system is usually limited by the maximum power. This partially explains a non-null mean temperature deviation. In the other case, the cooling system is rarely used because of his low efficiency.

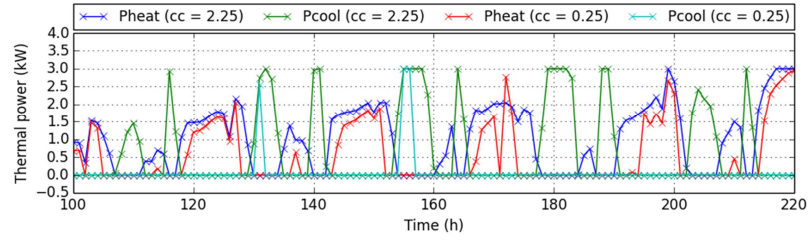


Figure 6 Heating and cooling optimal controls for $cc = 0.25$ and 2.25 (euros/°C/h)

Figure 7 presents the sold/bough power from the grid.

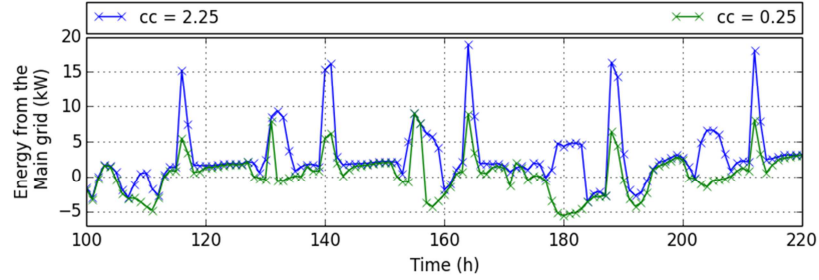


Figure 7 : Sold and bough power to/from the main grid for $cc = 0.25$ and 2.25 (euros/°C/h)

5.2. Pareto front of the multi-objective formulation

A set of 20 optimizations has been done for different costs of discomfort. Results are plotted in the Figure 8, each solution is represented by a point in the space Cost of Energy/Mean Discomfort.

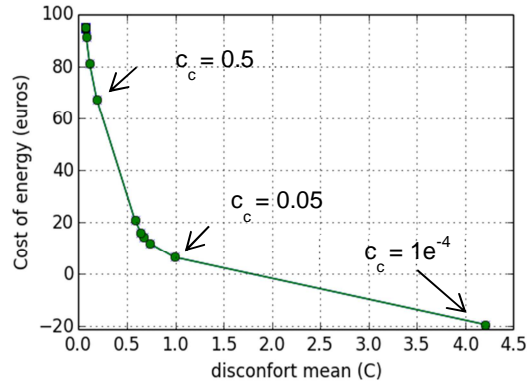


Figure 8 : Pareto front- cost of energy with respect to mean discomfort for $c_c = [1e^{-4}; 1000]$

We can observe that it exists two limitations in this Pareto's space. First, it is not possible to reach a perfect comfort (null discomfort) because of the limited heating and cooling systems. For the second limit, reached with a neglectable price of discomfort ($1e-4$), we observe a

maximal mean discomfort of 4.2 °C. Note that the cost of energy is negative for a discomfort mean up to 2°C.

6. Conclusions

A mixed-integer linear programming model of a smart building has been presented in this paper. This approach is tested for simple microgrid and thermal envelope of a building. A multi-objective formulation taking into account the price of energy and the thermal comfort has been discussed in this paper. The first quantitative results show the important role of the thermal capacity in the energy management and underline the compromise between the thermal discomfort and the price of energy.

7. Acknowledgements

The research leading to these results has received funding from the People Programme (Marie Curie Actions) of the European Union's Seventh Framework Programme FP7/2007-2013/ under project ELECON - Electricity Consumption Analysis to Promote Energy Efficiency Considering Demand Response and Non-technical Losses, REA grant agreement No 318912.

This work is also supported by FEDER Funds through the “Programa Operacional Factores de Competitividade – COMPETE” program and by National Funds through FCT “Fundação para a Ciência e a Tecnologia” under the projects FCOMP-01-0124-FEDER: PEst-OE/EEI/ UI0760/2011, PTDC/EEA-EEL/099832/2008, PTDC/ SEN-ENR/099844/2008, and PTDC/SEN-ENR/ 122174/2010; and SFRH/BD/80183/2011 (P. Faria PhD).

References

- [1] R. H. Lasseter, A. Akhil, C. Marnay, J. Stephens, J. Dagle, R. Guttromson, A. Meliopoulos, R. Yinger, and J. Eto, White Paper on Integration of Distributed Energy Resources: The CERTS MicroGrid Concept, Consortium for Electric Reliability Technology Solutions (CERTS), CA, Tech. Re LBNL-50829, 2002.
- [2] B. Buchholz and U. Schluecking, Energy management in distribution grids: European cases, IEEE Power Engineering Society General Meeting, (2006) 1-2.
- [3] F. Katiraei, R. Iravani, N. Hatziargyriou, and A. Dimeas, Microgrids management: Controls and operation aspects of microgrids, IEEE Power and Energy Magazine 6(3) (2008) 54-65.
- [4] S. X. Chen, H.B.Gooi, and M. Q. Wang, Sizing of Energy Storage for Microgrids, IEEE Transactions on smart grid, vol. 3, no. 1, march 2012, pp. 142-151
- [5] FICO, T. M. Xpress Optimization Suite. *Xpress-Optimizer, Reference manual*, 2009.
- [6] C. Klessmann, A. Held, M. Rathmann, M. Ragwitz, “Status and perspectives of renewable energy policy and deployment in the European Union—What is needed to reach the 2020 targets?”, Energy Policy, Vol. 39, no. 12, pp. 7637-7657, December 2011.
- [7] C. Tao, D. Shanxu, and C. Changsong, “Forecasting power output for grid-connected photovoltaic

- power system without using solar radiation measurement,” in *Proc. 2nd IEEE Int. Symp. Power Electron. Distrib. Gener. Syst. (PEDG)*, Jun. 2010, pp. 773–777
- [8] A. Yona, T. Senjyu, and T. Funabashi, “Application of recurrent neural network to short-term-ahead generating power forecasting for photovoltaic system,” in *Proc. Power Energy Soc. Gen. Meet.*, Jun. 2007, pp. 1–6.
- [9] B. Borowy and Z. Salameh, “Optimum photovoltaic array size for a hybrid wind/pv system,” *IEEE Trans. Energy Convers.*, vol. 9, no. 3, pp. 482–488, Sep. 1994.